Neuron
Report

Optogenetic Countering of Glial Acidosis Suppresses Glial Glutamate Release and Ischemic Brain Damage

Kaoru Beppu,[1,2,8] Takuya Sasaki,[1,8] Kenji F. Tanaka,[3] Akihiro Yamanaka,[4] Yugo Fukazawa,[5] Ryuichi Shigemoto,[1,2,6] and Ko Matsui[1,2,7,*]
[1]Division of Cerebral Structure, National Institute for Physiological Sciences
[2]Department of Physiological Sciences
Graduate University for Advanced Studies (SOKENDAI), Okazaki 444-8787, Japan
[3]Department of Neuropsychiatry, School of Medicine, Keio University, Tokyo 160-8582, Japan
[4]Department of Neuroscience II, Research Institute of Environmental Medicine, Nagoya University, Nagoya 464-8601, Japan
[5]Department of Anatomy and Molecular Cell Biology, Nagoya University Graduate School of Medicine, Nagoya 466-8550, Japan
[6]IST Austria, 3400 Klosterneuburg, Austria
[7]Division of Interdisciplinary Medical Science, Center for Neuroscience, Tohoku University Graduate School of Medicine, Sendai 980-8575, Japan
[8]These authors contributed equally to this work
*Correspondence: matsui@med.tohoku.ac.jp
http://dx.doi.org/10.1016/j.neuron.2013.11.011

SUMMARY

The brain demands high-energy supply and obstruction of blood flow causes rapid deterioration of the healthiness of brain cells. Two major events occur upon ischemia: acidosis and liberation of excess glutamate, which leads to excitotoxicity. However, cellular source of glutamate and its release mechanism upon ischemia remained unknown. Here we show a causal relationship between glial acidosis and neuronal excitotoxicity. As the major cation that flows through channelrhodopsin-2 (ChR2) is proton, this could be regarded as an optogenetic tool for instant intracellular acidification. Optical activation of ChR2 expressed in glial cells led to glial acidification and to release of glutamate. On the other hand, glial alkalization via optogenetic activation of a proton pump, archaerhodopsin (ArchT), led to cessation of glutamate release and to the relief of ischemic brain damage in vivo. Our results suggest that controlling glial pH may be an effective therapeutic strategy for intervention of ischemic brain damage.

INTRODUCTION

Upon brain ischemia, application of thrombolytic agents to induce reperfusion is the only effective therapeutic intervention proven. Liberation of excess glutamate upon ischemia is the direct trigger of neuronal cell death; however, as the cellular source of glutamate and its release mechanism were unidentified, targeted intervention to suppress glutamate release has mostly been unsuccessful (but see Hines and Haydon, 2013). We focused on the astrocytes of the glial cell population as they are the first responders to ischemic stress (Rossi et al., 2007). When aerobic metabolism shuts down as a consequence of oxygen and glucose deprivation, lactate production from glycogen stored predominantly in glial cells continues (Cataldo and Broadwell, 1986; Schurr et al., 1997), which leads to severe acidosis (Mutch and Hansen, 1984). Neuronal cell death via glutamate excitotoxicity follows (Lau and Tymianski, 2010). We simply connected these two events and hypothesized that glial acidosis triggers glial glutamate release. Based on this hypothesis, we sought an optogenetic intervention to control glutamate release upon ischemia and to understand the cellular mechanisms leading to its excess release.

RESULTS

OGD Induces Glutamate Release and Acidosis

Using acute cerebellar brain slices, ischemia was mimicked by oxygen and glucose deprivation (OGD) from continuously perfused artificial cerebrospinal fluid (ACSF) (Hamann et al., 2005). Neuronal cell health was monitored by whole-cell patch-clamp recordings from Purkinje cells (PCs) (Figure 1A). Shortly after the onset of OGD, transient burst firing occurred, which was followed closely by a plateau depolarization. These events could be considered as preludes to the eventual death of neurons. To monitor the excitatory drive evoked by OGD in isolation, we recorded PCs in voltage clamp and applied picrotoxin (PIC) to block inhibitory $GABA_A$ receptors. To exclude effects from neuronal transmitter release and focus on the glial contribution to ischemic stress, we also applied tetrodotoxin (TTX) and Cd^{2+} to block action potentials and voltage-gated Ca^{2+} channels, respectively. Within minutes, inward current developed, suggesting that OGD triggered release of excitatory substance from nonsynaptic sources, presumably from glia (Figure 1B). Whether this inward current is evoked by glutamate was examined with an AMPA receptor blocker alone (GYKI) or with a cocktail of glutamate receptor and transporter (GluR/T)

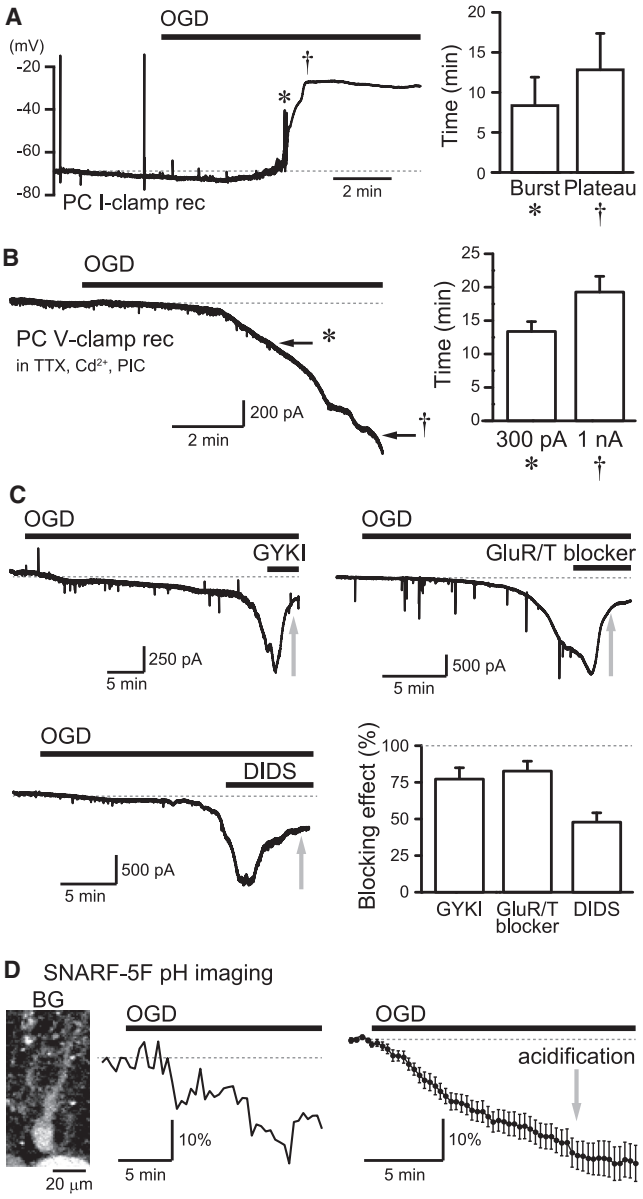

Figure 1. Ischemic Stress Produced Glial Acidosis and Glutamate Release

(A) Upon OGD, PCs displayed transient burst firing (*), followed by depolarization to a plateau (†). Average time of each event from the OGD onset is shown (right; burst, n = 5; plateau, n = 6). (B) Excitatory current developed upon OGD in the presence of TTX, Cd^{2+}, and PIC. Average time to reach –300 pA (*, n = 22) and –1 nA (†, n = 14) is shown (right). (C) An AMPA receptor blocker (all units in μM) (100 GYKI53655), glutamate receptor and transporter blockers (10 NBQX, 200 D-AP5, 100 LY363785, 50 TBOA), or an anion channel blocker (1,000 DIDS) suppressed OGD-induced PC-current (GYKI, *$p < 0.01$, n = 6; GluR/T blocker, *$p < 0.01$, n = 9; DIDS, *$p < 0.01$, n = 8). The DIDS effect was variable between cells (min = 22.8, max = 96.5%). (D) A representative BG stained with SNARF-5F (left) and the fluorescence change upon OGD, indicating intracellular acidification (middle). Average trace, right (n = 14). Recordings in (B), (C), and (D) were in the presence of TTX, Cd^{2+}, and PIC. Error bars represent SEM. See also Figure S1.

blockers (NBQX, D-AP5, LY363785, and TBOA) (Figure 1C). OGD-induced inward current was significantly blocked in both cases, demonstrating that the majority of the inward current is due to glutamate. It should be noted, however, that some current remained, suggesting that OGD also triggers effects other than glutamate release. Our previous report has suggested that glial glutamate release can occur through 4,4'-diisothiocyanostilbene-2,2′-disulphonic acid (DIDS)-sensitive anion channels (Sasaki et al., 2012). Application of DIDS also partially inhibited the OGD-induced inward currents. These results suggest that release through DIDS-sensitive mechanisms could be one of the primary sources of excess glutamate liberation upon ischemia (Camacho et al., 2006; Liu et al., 2006; Seki et al., 1999), although DIDS-insensitive mechanisms also likely have a role. It has also been reported that glutamate release can occur through reversal of glutamate transporters. Extracellular TBOA has been suggested to block glutamate transporter reversal (Phillis et al., 2000); however, the development of the OGD-induced current was only accelerated by TBOA (Figure S1A available online), likely due to the slower clearance of the released glutamate by blocking of the uptake by TBOA. Therefore, we were unable to assess the relative contributions of each component of glutamate release mechanisms.

Based on previous reports indicating the presence of pH-dependent anion channels that are DIDS sensitive (Cavelier and Attwell, 2005; Lambert and Oberwinkler, 2005; Zifarelli et al., 2008) and pH-dependent amino acid transporters (Sakai et al., 2003; Weiss et al., 2005), we next sought to examine the causal link between glial acidification and glutamate release. First, we verified that glial acidification indeed occurs upon OGD in acute cerebellar slices by using a pH-sensitive fluorescence dye, SNARF-5F AM (Figure 1D and Figures S1B and S1C). OGD elicited rapid reduction of SNARF-5F fluorescence ratio in cerebellar Bergmann glial cells (BGs), indicating intracellular acidification. Cells other than BGs were also acidified and the time course of acidification was examined in granule cells (GCs), which have similar soma size as the BGs. Interestingly, the onset of acidification was significantly faster in BGs than GCs (Figures S1D and S1E).

Acidification Is the Trigger for Glial Glutamate Release

We next attempted to bypass the OGD process and directly acidify glial cells by optogenetic activation of ChR2. ChR2 is a light-sensitive cation channel and it is usually considered as a tool to optically excite cell activity via membrane depolarization. However, contrary to other excitatory channels such as Na^+ channels or ionotropic glutamate receptor channels, ChR2 has much more permeability to H^+ than Na^+ (Nagel et al., 2003). Thus, ChR2 could be considered as an optogenetic tool for manipulation of intracellular pH. We employed a transgenic mouse line in which highly light-sensitive mutant (C128S [Berndt et al., 2009]) of ChR2 was selectively expressed in astrocytes including BGs using the tetracycline transactivator (tTA)-tet operator (tetO) system (Tanaka et al., 2012). To confirm proton influx by ChR2 opening, we measured photocurrents from BGs with intracellular and extracellular cations mostly replaced with N-Methyl-D-glucamine (NMDG), a cation with little permeability to ChR2; thus, the only cation left permeable was proton

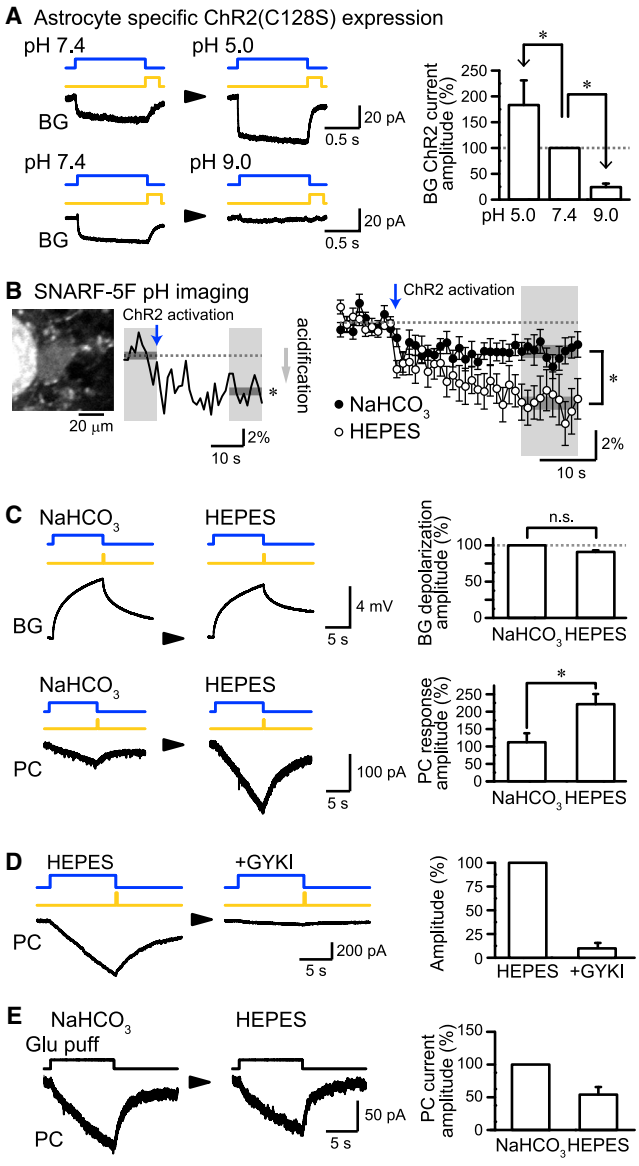

Figure 2. Acidification Is the Trigger for Glial Glutamate Release

(A) Astrocyte-specific ChR2(C128S)-expressing mice were used. H^+ permeability of ChR2(C128S) expressed on BGs was assessed by changing the extracellular pH from 7.4 to 5.0 (top) or 9.0 (bottom). Photocurrent amplitude at 100–200 ms from the blue light onset was significantly increased in pH 5.0 (*$p < 0.01$, $n = 5$, paired t test) and decreased in pH 9.0 (*$p < 0.01$, $n = 8$, paired t test). Blue and yellow light opens and closes the ChR2(C128S) channel, respectively. (B) pH imaging of BGs with SNARF-5F. A single pulse of blue light opened the ChR2(C128S) channel for a prolonged time and intracellular acidification was induced. The acidification was stronger in HEPES compared to $NaHCO_3$ external buffer (*$p < 0.01$, $n = 12$ each, Student's t test). (C) BG depolarization amplitude via ChR2(C128S) photoactivation was not affected by the external pH buffer ($p = 0.07$, $n = 3$, paired t test, top), whereas glial ChR2-photoactivated PC currents became significantly larger by altering the buffer from $NaHCO_3$ to HEPES compared to $NaHCO_3$ to $NaHCO_3$ (*$p < 0.05$, $n = 7$ and 3, Student's t test). (D) Application of GYKI, an AMPA receptor-specific antagonist, blocked glial ChR2-photoactivated PC current in HEPES-based solution. (E) Exchanging the extracellular solution from $NaHCO_3$-based to HEPES-based buffer did not increase PC currents in response to glutamate (200 μM) puff application ($n = 5$) but rather decreased it. Although we are uncertain about the mechanism underlying this decrease, this result indicates that the increase in the glial ChR2-photoactivated PC current upon exchanging the extracellular solutions (Figure 2C) was not due to the increase in the glutamate sensitivity of PC glutamate receptors. All recordings were in TTX, Cd^{2+}, and PIC. Error bars represent SEM. See also Figure S2.

(Figure 2A). Decreasing pH means increasing proton concentration. Decreasing the external pH from 7.4 to 5.0 enhanced the photocurrent, whereas increasing the pH from 7.4 to 9.0 reduced it. These data suggest that our C128S-modified ChR2 expressed in BGs are also permeable to proton, although it is possible that ChR2 channel opening itself could be regulated by external pH. To verify proton influx through ChR2(C128S) in normal intracellular and extracellular solutions, we performed pH imaging, and BG acidification by ChR2(C128S) photoactivation was confirmed (Figure 2B). These results indicate that proton influx occurs upon ChR2 activation; however, if trace amount of ChR2 is also expressed in intracellular compartments, proton could enter the cytosol from these sources as well (Gourine et al., 2010).

We have shown previously that glial ChR2 photoactivation resulted in glutamate release that could be detected as AMPA receptor-mediated current in PCs (Sasaki et al., 2012). Considering the above results, it is possible that proton influx direct triggers glutamate release; however, it is also possible that depolarization itself caused by the ChR2 photoactivation or the very small amount of Ca^{2+} influx via ChR2 openings could be the actual trigger. Therefore, we devised a way to cause different amounts of acidification with the same amount of proton influx by manipulating the intracellular pH buffering capacity. Intracellular pH is considered to be buffered by HCO_3^- and depriving extracellular HCO_3^- would probably cause efflux of intracellular HCO_3^- and result in low buffering capacity of the intracellular pH (Zhang et al., 2010). Consistent with this idea, acidification measured by SNARF-5F imaging was significantly stronger in extracellular 5 mM HEPES buffer solution compared with extracellular $NaHCO_3$ buffer solution, even though both solutions were adjusted to the same pH (Figure 2B, right). No significant difference was found in the amplitude of ChR2-induced BG depolarization upon switching from $NaHCO_3$-based to HEPES-based solution (Figure 2C, top); however, glial ChR2-photoactivated PC current was significantly increased (Figure 2C, bottom). The PC current in HEPES was mostly blocked by GYKI (Figure 2D), as in the normal $NaHCO_3$ solution (Sasaki et al., 2012). No current was induced with photostimulation in BGs or PCs from mice that lack the expression of optogenetic tools (Figure S2A). Glutamate sensitivity of PC currents was not increased by switching the external solutions (Figure 2E). These observations imply that stronger intracellular glial acidification leads to larger amount of glutamate release. To test the H^+-triggered glutamate release hypothesis further, we employed an alternative method to induce intracellular acidification, which was to locally pressure (puff) apply a weak membrane-permeable acid, acetate. This did not induce depolarization of BGs but did evoke a slow inward current in PCs, which was not detected in the presence of GYKI (Figure S2B). To further exclude

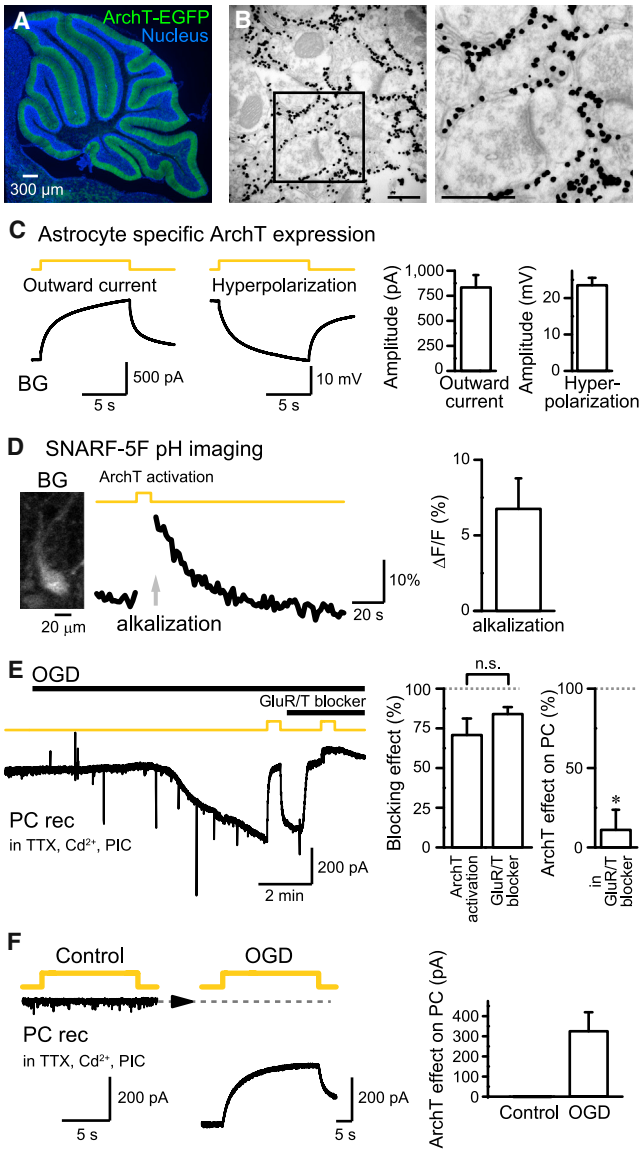

Figure 3. Glial Alkalization Suppressed OGD-Induced PC Currents

(A) Astrocyte-specific ArchT-expressing mice were used. The bigenic mice, Mlc1-tTA::tetO-ArchT-EGFP, express ArchT selectively in astrocytes in cerebellar cortex. Blue, nuclear staining by H33342; green, EGFP fluorescence. (B) Immunogold EM of EGFP in the bigenic mice. EGFP was confirmed to be localized only in the astrocytes (288, 0, 0, and 1 immunogolds in identified astrocyte, presynaptic, postsynaptic, and unidentifiable profiles, respectively). Scale bars indicate 500 nm in low- (left) and high- (right) magnified images. (C) Typical current (left) and voltage (right) responses of BGs to ArchT photoactivation (yellow). Right: average amplitudes of outward current (n = 9) and hyperpolarization (n = 6). (D) pH imaging of a BG showed that alkalization was induced with glial ArchT photoactivation. Right: results summarized (n = 7). (E) OGD-induced PC currents were reduced by glial ArchT photoactivation (time constant to reach equilibrium = 1.6 ± 0.2 s, n = 8). The effect was not significantly different from the blocking effect of GluR/T blockers (p = 0.27, n = 8, 14, Student's t test). ArchT photoactivation effect on PC was significantly reduced in the presence of GluR/T blockers (*p < 0.05, n = 5, paired t test). (F) Glial ArchT-photoactivated PC currents were not detected under control condition, whereas the glial ArchT photoactivation generated outward PC currents during OGD. Average amplitudes of the outward current (9.5–10 s after yellow light application) were summarized (n = 7 each). Recordings in (D), (E), and (F) were in the presence of TTX, Cd^{2+}, and PIC. Error bars represent SEM. See also Figure S3.

depolarization as the primary trigger of glial glutamate release, we examined the effect of puff application of high concentration of K^+. Similar to ChR2 photoactivation, high K^+ application caused BG depolarization, but the current recorded from PCs was not altered by application of GYKI or NBQX (Figure S2C); thus, glutamate is not likely to be released as a consequence of BG depolarization or by high extracellular K^+ in the presence of TTX and Cd^{2+}. The Ca^{2+} permeability of ChR2 is very low unless it is specifically modified (Kleinlogel et al., 2011; Li et al., 2012); thus, Ca^{2+} influx through these channels is not likely to be sufficient to drive glial glutamate release (Woo et al., 2012). To verify this idea, we omitted Ca^{2+} and added EGTA to the extracellular solution. The glial ChR2-photoactivated PC current remained uninhibited in this condition (Figure S2D). It is still possible that intracellular Ca^{2+} increase could occur subsequent to intracellular acidification (Orlowski et al., 2011). To evaluate whether Ca^{2+} is involved in the signaling pathway, we strongly buffered intracellular Ca^{2+} with BAPTA-AM. Although BAPTA-AM was sufficient to strongly suppress neuronal synaptic release of glutamate (Figure S2E), it did not significantly alter glial ChR2-photoactivated PC currents (Figure S2F). It still remains possible that coupling between Ca^{2+} source and glutamate release mechanisms is even tighter in glial cells than in synapses; thus, we could not completely exclude the role of Ca^{2+} as the intermediate of acidification and glutamate release.

Countering Glial Acidosis Inhibits Neuronal Damage

If glial acidification were the key trigger of glutamate release upon ischemia, countering acidification with alkalization should be able to inhibit glutamate release and excitotoxicity. To selectively increase glial intracellular pH, we generated a mouse line in which astrocyte population of glia, including BGs, specifically expresses ArchT, a light-sensitive outward proton pump (Han et al., 2011) using the tTA-tetO system (Tsunematsu et al., 2013). Immunofluorescence and immunogold electron microscopic observations confirmed specific expression of ArchT in BGs (Figures 3A and 3B and Figure S3A). ArchT photoactivation produced outward currents and hyperpolarization in BGs in voltage- and current-clamp modes, respectively (Figure 3C). pH imaging also showed that ArchT photoactivation reliably induced alkalization of BGs (Figure 3D). Glial ArchT photoactivation dramatically inhibited OGD-induced inward currents in PCs (Figure 3E). Similar results were obtained at near-physiological temperature (Figure S3B). Glial ArchT photoactivation alone in control condition did not evoke any current in PCs and the effect was only evident in OGD (Figure 3F); thus, proton efflux from glia or other ionic change does not directly produce any current in PCs. Furthermore, the blocking effect of glial ArchT photoactivation on OGD-induced PC currents was nearly equal to that of GluR/T blocker application (Figure 3E, middle) and was occluded in the presence of GluR/T blockade (Figure 3E, right). As DIDS could only block half of the OGD-induced current (Figure 1C) and, as the ArchT effect was only partially occluded by DIDS (Figure S3C), there likely exists DIDS-sensitive and -insensitive

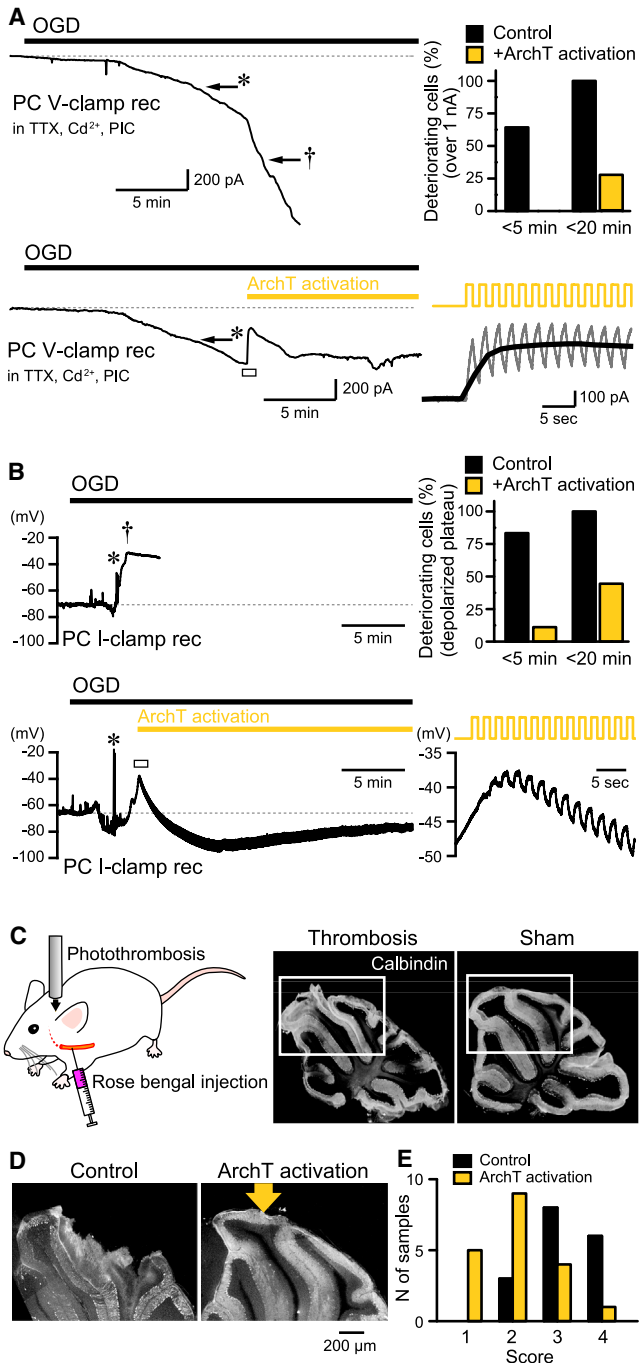

Figure 4. Glial Alkalization by ArchT Photoactivation Relieved Ischemic Brain Damage

(A) OGD-induced PC-currents without (top) and with (bottom) intermittent glial ArchT photoactivation. PC currents reaching –300 pA and –1 nA are indicated by * and †, respectively. Percentage of cells displaying inward currents of >1 nA within the time indicated is summarized (right). The bottom trace (boxed area) is magnified on right and the current trace before decimating the data points is shown in gray. (B) Current-clamp recording from PCs without (top) and with (bottom) intermittent glial ArchT photoactivation. Transient burst firing and the onset of plateau depolarization are indicated by * and †, respectively. Percentage of cells reaching plateau depolarization is summarized (right). The bottom trace (boxed area) is magnified on right. (C) Left: schematic illustration of the creation of cerebellar ischemia with artificial thrombosis. Right: typical images of calbindin immunostaining of the cerebellum in a rose bengal-injected (Thrombosis) and noninjected mouse (Sham). Boxes indicate the approximate region of illumination. (D) Representative images of cerebellum from astrocyte-specific ArchT-expressing mice not exposed (left) and exposed (right) to intermittent glial ArchT photoactivation. (E) Scores of ischemic brain damage with higher numbers indicating more severe damage (n = 17 and 19 mice, $p < 0.01$, Wilcoxon ranked-sum test). See also Figure S4.

glial glutamate release mechanisms, both of which are pH sensitive. As glutamate uptake by glutamate transporters is voltage dependent (Bergles et al., 1997), it is possible that glutamate release is not suppressed but the uptake is facilitated in glia, which is hyperpolarized by ArchT photoactivation. To examine this possibility, we induced OGD in the presence of TBOA. Glial ArchT photoactivation blocked OGD-induced PC currents similarly, even in the presence of TBOA (Figure S3D). Taken together, these data suggest that glial pH change is an upstream causal factor of glutamate release upon ischemia.

We next examined whether intermittent glial ArchT photoactivation could prevent deterioration of the healthiness of neurons upon ischemia. Excitatory drive recorded from PCs in voltage clamp rapidly increased upon OGD and over 1 nA of inward current was observed within 20 min. We next introduced intermittent glial ArchT photoactivation after detecting inward currents of more than 300 pA. Further development of inward current was prominently suppressed (Figure 4A). The inward current could not be suppressed completely, suggesting the presence of additional unidentified mechanisms that lead to the increased conductance. Similarly, in current-clamp recordings from PCs in the absence of pharmacological agents, glial ArchT photoactivation was introduced after burst firing emerged upon OGD (Figure 4B). Without the photoactivation, PCs soon reached plateau depolarization, whereas photoactivation suppressed this indication of cell deterioration.

Could simply countering acidosis with glial alkalization exert a neuroprotective action upon ischemia? To answer this question, ischemia in the cerebellum in vivo was created by using a photosensitive dye, rose bengal (Watson et al., 1985). Rose bengal was injected intra-arterially and focal ischemic region was created by exciting this dye via an optic fiber placed above the cerebellum and thrombosis was artificially created. Three hours after creation of thrombosis, severe neuronal degeneration was confirmed (Figure 4C). To quantify the level of damage, we scored brain sections based on the relative loss of PCs and the degenerated area (Figure S4). In one group of mice, glial ArchT photoactivation was intermittently applied from 0.5 to 2.5 hr after the creation of thrombosis. In this group, progressive generation of infarct area was significantly inhibited at 3 hr from photothrombosis (Figures 4D and 4E). These results demonstrate that countering of astrocyte acidosis can reduce brain damage upon ischemia.

DISCUSSION

Evidence for glia modulating neuronal activity (Panatier et al., 2011; Saab et al., 2012) and glutamate being used as gliotransmitter is accumulating (Woo et al., 2012); however, the

mechanism of its release remains to be elucidated. Several reports have indicated that the release is Ca^{2+} dependent (Halassa and Haydon, 2010), although functional significance of glial Ca^{2+} has also been questioned (Agulhon et al., 2010; Sun et al., 2013). Here, we propose that glial pH changes are a significant regulator of glutamate release in the cerebellum. We focused on the cerebellum because of the close morphological apposition of glial and neuronal elements that suggests that, if there is any commitment of glial cell activities in physiological or pathophysiological circumstances, it could manifest most in the cerebellum. As pH-dependent glial ATP release has also been shown (Gourine et al., 2010), pH could be a key glial intracellular signal, which is as pivotal as Ca^{2+}, although the relative importance of pH may differ among different brain regions (Kasymov et al., 2013).

It should be noted that we are not proposing that H^+-triggered glial glutamate release is the only mechanism underlying liberation of excess glutamate upon ischemia. Most of the current experiments were done in TTX and Cd^{2+} to focus on the glial component, but neurons have also been shown to release glutamate during the initial stage of ischemia by vesicular release, and reversal of neuronal and glial glutamate transporters has also been shown to occur (Gebhardt et al., 2002; Hamann et al., 2005; Rossi et al., 2007). The relative role of each component is difficult to assess, as blocking one component will also disrupt the interplay between all components. However, our data do show that suppression of glial glutamate release alone by glial ArchT photoactivation can sustain hyperpolarization of neurons in half of the cells in slices in the absence of all pharmacological agents for some time (Figure 4B) and save the brain from large structural damage in vivo (Figure 4D).

Direct application of our findings in patients is limited, as it would require preemptive gene therapy before ischemia. However, our data do show that countering of glial acidosis alone can powerfully suppress ischemic brain damage, which suggests that pH-dependent glial glutamate release is one of the pathways leading to excitotoxic cell death. Therapeutic strategy could involve simple delivering of cell-permeable strong pH buffer or pharmacological agents directed to facilitate H^+ exchange. As glial ChR2-photoactivated PC current was not sensitive to NPPB (Sasaki et al., 2012), the glutamate release mechanism is not likely to be via Best1 (Woo et al., 2012). Other various anion channels and transporters have been reported to deliver glutamate to extracellular space with different pharmacological characteristics (Fields and Ni, 2010); however, most of their molecular identity has not been specified. If we are able to find which channel or transporter is involved in the pH-dependent glial glutamate release, targeted drug design would become plausible.

EXPERIMENTAL PROCEDURES

All experiments were performed in accordance with the guidelines of the Physiological Society of Japan.

Electrophysiology

Acute slice preparation and whole-cell patch-clamp recording were performed as described previously (Sasaki et al., 2012). To simulate energy deprivation upon brain ischemia, we omitted glucose and superfusate bubbled with 95% N_2, 5% CO_2 was used. For most experiments, photostimulation was delivered to the slices through the objective lens, but for the ArchT activation during pH imaging, photostimulation was given through the condenser lens as described in the Supplemental Experimental Procedures.

pH Imaging

Cells were loaded with local puff application of SNARF-5F AM. In most recordings, SNARF-5F was excited with 810 nm two-photon laser and fluorescence was detected using two emission filters (586/20 nm and 650/60 nm) and the fluorescence ratio ($R_{650/586}$) was calculated. Details are described in Supplemental Experimental Procedures.

Optogenetic Mice

tetO-ChR2(C128S)-EYFP β-actin gene locus knockin mice (Tanaka et al., 2012), tetO-ArchT-EGFP β-actin gene BAC transgenic mice (Tsunematsu et al., 2013), and astrocyte specific Mlc1-tTA mice (Sasaki et al., 2012; Tanaka et al., 2010) were used. Bigenic mice were created by crossing the Mlc1-tTA with either of the tetO lines. Details are described in the Supplemental Experimental Procedures.

Immunogold Electron Microscopy of Mlc1-tTA::tetO-ArchT-EGFP Mice

Tissue processing for preembedding immunoelectron microscopy was performed as described previously (Parajuli et al., 2012). Mouse anti-GFP antibody (1 μg/ml, Clone mFX73, Wako) was used as a primary antibody, and enhancement of the immunogold particles was carried out by using a gold enhance-EM kit (Nanoprobes). Details are described in the Supplemental Experimental Procedures.

Creation of Cerebellar Ischemia Model and In Vivo Glial ArchT Photoactivation

Rose bengal was administrated through the left carotid artery (Watson et al., 1985) and the dye was excited for 4–5 min via an optical fiber placed just above the craniotomy made over the cerebellum. A group of mice was given intermittent glial ArchT photoactivation (1 s light on, 1 s light off cycle for 2.5 hr), which started after 30 min from the photothrombosis. The mice were sacrificed after 3 hr from the photothrombosis. Details of the evaluation of the infarct area are described in the Supplemental Experimental Procedures.

SUPPLEMENTAL INFORMATION

Supplemental Information includes Supplemental Experimental Procedures and four figures and can be found with this article online at http://dx.doi.org/10.1016/j.neuron.2013.11.011.

ACKNOWLEDGMENTS

This work was supported by grants from Grant-in-Aid for Scientific Research on Innovative Areas "Mesoscopic Neurocircuitry" and "Comprehensive Brain Science Network" from the Ministry of Education, Culture, Sports, Science and Technology of Japan (MEXT) to K.M. (25115729), A.Y. (23115103), and Y.F. (23115520), Grant-in-Aid for Young Scientists (A) from MEXT to K.M. (25702054) and K.F.T. (23680042), Takeda Science Foundation to K.M., K.F.T., and A.Y., and Grant-in-Aid for Scientific Research (B) from MEXT to A.Y. (23300142). We thank Dr. Tomomi Tsunematsu, Claire Saito, and Keiko Nishimura for technical assistance and Norifumi Shioda for useful suggestion for creating ischemia in mice.

Accepted: October 31, 2013
Published: January 22, 2014

REFERENCES

Agulhon, C., Fiacco, T.A., and McCarthy, K.D. (2010). Hippocampal short- and long-term plasticity are not modulated by astrocyte Ca2+ signaling. Science *327*, 1250–1254.

Bergles, D.E., Dzubay, J.A., and Jahr, C.E. (1997). Glutamate transporter currents in bergmann glial cells follow the time course of extrasynaptic glutamate. Proc. Natl. Acad. Sci. USA *94*, 14821–14825.

Berndt, A., Yizhar, O., Gunaydin, L.A., Hegemann, P., and Deisseroth, K. (2009). Bi-stable neural state switches. Nat. Neurosci. *12*, 229–234.

Camacho, A., Montiel, T., and Massieu, L. (2006). The anion channel blocker, 4,4′-dinitrostilbene-2,2′-disulfonic acid prevents neuronal death and excitatory amino acid release during glycolysis inhibition in the hippocampus in vivo. Neuroscience *142*, 1005–1017.

Cataldo, A.M., and Broadwell, R.D. (1986). Cytochemical identification of cerebral glycogen and glucose-6-phosphatase activity under normal and experimental conditions. II. Choroid plexus and ependymal epithelia, endothelia and pericytes. J. Neurocytol. *15*, 511–524.

Cavelier, P., and Attwell, D. (2005). Tonic release of glutamate by a DIDS-sensitive mechanism in rat hippocampal slices. J. Physiol. *564*, 397–410.

Fields, R.D., and Ni, Y. (2010). Nonsynaptic communication through ATP release from volume-activated anion channels in axons. Sci. Signal. *3*, ra73.

Gebhardt, C., Körner, R., and Heinemann, U. (2002). Delayed anoxic depolarizations in hippocampal neurons of mice lacking the excitatory amino acid carrier 1. J. Cereb. Blood Flow Metab. *22*, 569–575.

Gourine, A.V., Kasymov, V., Marina, N., Tang, F., Figueiredo, M.F., Lane, S., Teschemacher, A.G., Spyer, K.M., Deisseroth, K., and Kasparov, S. (2010). Astrocytes control breathing through pH-dependent release of ATP. Science *329*, 571–575.

Halassa, M.M., and Haydon, P.G. (2010). Integrated brain circuits: astrocytic networks modulate neuronal activity and behavior. Annu. Rev. Physiol. *72*, 335–355.

Hamann, M., Rossi, D.J., Mohr, C., Andrade, A.L., and Attwell, D. (2005). The electrical response of cerebellar Purkinje neurons to simulated ischaemia. Brain *128*, 2408–2420.

Han, X., Chow, B.Y., Zhou, H., Klapoetke, N.C., Chuong, A., Rajimehr, R., Yang, A., Baratta, M.V., Winkle, J., Desimone, R., and Boyden, E.S. (2011). A high-light sensitivity optical neural silencer: development and application to optogenetic control of non-human primate cortex. Front. Syst. Neurosci. *5*, 18.

Hines, D.J., and Haydon, P.G. (2013). Inhibition of a SNARE-sensitive pathway in astrocytes attenuates damage following stroke. J. Neurosci. *33*, 4234–4240.

Kasymov, V., Larina, O., Castaldo, C., Marina, N., Patrushev, M., Kasparov, S., and Gourine, A.V. (2013). Differential sensitivity of brainstem versus cortical astrocytes to changes in pH reveals functional regional specialization of astroglia. J. Neurosci. *33*, 435–441.

Kleinlogel, S., Feldbauer, K., Dempski, R.E., Fotis, H., Wood, P.G., Bamann, C., and Bamberg, E. (2011). Ultra light-sensitive and fast neuronal activation with the Ca^{2+}-permeable channelrhodopsin CatCh. Nat. Neurosci. *14*, 513–518.

Lambert, S., and Oberwinkler, J. (2005). Characterization of a proton-activated, outwardly rectifying anion channel. J. Physiol. *567*, 191–213.

Lau, A., and Tymianski, M. (2010). Glutamate receptors, neurotoxicity and neurodegeneration. Pflugers Arch. *460*, 525–542.

Li, D., Hérault, K., Isacoff, E.Y., Oheim, M., and Ropert, N. (2012). Optogenetic activation of LiGluR-expressing astrocytes evokes anion channel-mediated glutamate release. J. Physiol. *590*, 855–873.

Liu, H.T., Tashmukhamedov, B.A., Inoue, H., Okada, Y., and Sabirov, R.Z. (2006). Roles of two types of anion channels in glutamate release from mouse astrocytes under ischemic or osmotic stress. Glia *54*, 343–357.

Mutch, W.A., and Hansen, A.J. (1984). Extracellular pH changes during spreading depression and cerebral ischemia: mechanisms of brain pH regulation. J. Cereb. Blood Flow Metab. *4*, 17–27.

Nagel, G., Szellas, T., Huhn, W., Kateriya, S., Adeishvili, N., Berthold, P., Ollig, D., Hegemann, P., and Bamberg, E. (2003). Channelrhodopsin-2, a directly light-gated cation-selective membrane channel. Proc. Natl. Acad. Sci. USA *100*, 13940–13945.

Orlowski, P., Chappell, M., Park, C.S., Grau, V., and Payne, S. (2011). Modelling of pH dynamics in brain cells after stroke. Interface Focus *1*, 408–416.

Panatier, A., Vallée, J., Haber, M., Murai, K.K., Lacaille, J.C., and Robitaille, R. (2011). Astrocytes are endogenous regulators of basal transmission at central synapses. Cell *146*, 785–798.

Parajuli, L.K., Nakajima, C., Kulik, A., Matsui, K., Schneider, T., Shigemoto, R., and Fukazawa, Y. (2012). Quantitative regional and ultrastructural localization of the Ca(v)2.3 subunit of R-type calcium channel in mouse brain. J. Neurosci. *32*, 13555–13567.

Phillis, J.W., Ren, J., and O'Regan, M.H. (2000). Transporter reversal as a mechanism of glutamate release from the ischemic rat cerebral cortex: studies with DL-threo-beta-benzyloxyaspartate. Brain Res. *868*, 105–112.

Rossi, D.J., Brady, J.D., and Mohr, C. (2007). Astrocyte metabolism and signaling during brain ischemia. Nat. Neurosci. *10*, 1377–1386.

Saab, A.S., Neumeyer, A., Jahn, H.M., Cupido, A., Šimek, A.A., Boele, H.J., Scheller, A., Le Meur, K., Götz, M., Monyer, H., et al. (2012). Bergmann glial AMPA receptors are required for fine motor coordination. Science *337*, 749–753.

Sakai, K., Shimizu, H., Koike, T., Furuya, S., and Watanabe, M. (2003). Neutral amino acid transporter ASCT1 is preferentially expressed in L-Ser-synthetic/storing glial cells in the mouse brain with transient expression in developing capillaries. J. Neurosci. *23*, 550–560.

Sasaki, T., Beppu, K., Tanaka, K.F., Fukazawa, Y., Shigemoto, R., and Matsui, K. (2012). Application of an optogenetic byway for perturbing neuronal activity via glial photostimulation. Proc. Natl. Acad. Sci. USA *109*, 20720–20725.

Schurr, A., Payne, R.S., Miller, J.J., and Rigor, B.M. (1997). Glia are the main source of lactate utilized by neurons for recovery of function posthypoxia. Brain Res. *774*, 221–224.

Seki, Y., Feustel, P.J., Keller, R.W., Jr., Tranmer, B.I., and Kimelberg, H.K. (1999). Inhibition of ischemia-induced glutamate release in rat striatum by dihydrokinate and an anion channel blocker. Stroke *30*, 433–440.

Sun, W., McConnell, E., Pare, J.F., Xu, Q., Chen, M., Peng, W., Lovatt, D., Han, X., Smith, Y., and Nedergaard, M. (2013). Glutamate-dependent neuroglial calcium signaling differs between young and adult brain. Science *339*, 197–200.

Tanaka, K.F., Ahmari, S.E., Leonardo, E.D., Richardson-Jones, J.W., Budreck, E.C., Scheiffele, P., Sugio, S., Inamura, N., Ikenaka, K., and Hen, R. (2010). Flexible Accelerated STOP Tetracycline Operator-knockin (FAST): a versatile and efficient new gene modulating system. Biol. Psychiatry *67*, 770–773.

Tanaka, K.F., Matsui, K., Sasaki, T., Sano, H., Sugio, S., Fan, K., Hen, R., Nakai, J., Yanagawa, Y., Hasuwa, H., et al. (2012). Expanding the repertoire of optogenetically targeted cells with an enhanced gene expression system. Cell Rep *2*, 397–406.

Tsunematsu, T., Tabuchi, S., Tanaka, K.F., Boyden, E.S., Tominaga, M., and Yamanaka, A. (2013). Long-lasting silencing of orexin/hypocretin neurons using archaerhodopsin induces slow-wave sleep in mice. Behav. Brain Res. *255*, 64–74.

Watson, B.D., Dietrich, W.D., Busto, R., Wachtel, M.S., and Ginsberg, M.D. (1985). Induction of reproducible brain infarction by photochemically initiated thrombosis. Ann. Neurol. *17*, 497–504.

Weiss, M.D., Rossignol, C., Sumners, C., and Anderson, K.J. (2005). A pH-dependent increase in neuronal glutamate efflux in vitro: possible involvement of ASCT1. Brain Res. *1056*, 105–112.

Woo, D.H., Han, K.S., Shim, J.W., Yoon, B.E., Kim, E., Bae, J.Y., Oh, S.J., Hwang, E.M., Marmorstein, A.D., Bae, Y.C., et al. (2012). TREK-1 and Best1 channels mediate fast and slow glutamate release in astrocytes upon GPCR activation. Cell *151*, 25–40.

Zhang, Z., Nguyen, K.T., Barrett, E.F., and David, G. (2010). Vesicular ATPase inserted into the plasma membrane of motor terminals by exocytosis alkalinizes cytosolic pH and facilitates endocytosis. Neuron *68*, 1097–1108.

Zifarelli, G., Murgia, A.R., Soliani, P., and Pusch, M. (2008). Intracellular proton regulation of ClC-0. J. Gen. Physiol. *132*, 185–198.